

# Review effect of various types of dyes and structures in supporting performance of dye- sensitized solar cell TiO<sub>2</sub>-based nanocomposites

*by*

---

**Submission date:** 20-May-2022 09:50PM (UTC+0700)

**Submission ID:** 1840678142

**File name:** 2022\_Fitria.pdf (1.93M)

**Word count:** 10271

**Character count:** 53450

# Review effect of various types of dyes and structures in supporting performance of dye-sensitized solar cell TiO<sub>2</sub>-based nanocomposites

Fitriah Mujtahid | Paulus Lobo Gareso | Bidayatul Arminyah | Dahlang Tahir 

Department of Physics, Hasanuddin University, Makassar, Indonesia

## Correspondence

Dahlang Tahir, Department of Physics, Hasanuddin University, Makassar 90245, Indonesia.

Email: dtahir@fmipa.unhas.ac.id

## Funding information

DIKTI/BRIN, Indonesia, Grant/Award Number: 752/UN4.22/PT.01.03/2021

## Summary

The energy demand for supporting the activity of human life is increasing where fossil fuels decreasing sharply every year and have an impact on increasing CO<sub>2</sub> emissions in the environment. An alternative solution for providing practical energy needs is using renewable energy such as solar cells. For environmentally friendly, economical, and efficient concepts, dye-sensitized solar cell (DSSC) is a promising alternative for the photovoltaic field. The performance of a DSSC depends on many factors, such as electron collection at the photoanode, photoanode light-harvesting efficiency, and others. In this review article, we observe the influence of synthetic and natural dye materials on light-harvesting efficiency at photoanodes. The chemical structure of dyes plays an essential role in increasing photon absorption, thereby increasing electron injection and conversion efficiency. In addition to dyes, we also reviewed the influence of the shape of the DSSC structure, namely the sandwich, monolithic, and honeycomb structures, on the performance of DSSCs. This approach helps develop a narrative about the potential and relationship of dyes and structure in increasing efficiency as a guide for synthesizing new materials in the future.

## KEYWORDS

dye-sensitized solar cell, natural dyes, structure, synthetic dye, TiO<sub>2</sub> nanocomposite

## 1 | INTRODUCTION

The utilization of the energy derived from fossil fuels impacts environmental pollution. The process of burning fossil fuels has an impact on increasing greenhouse gas emissions in the environment. To reduce the effect of using fossil fuels, efforts were made to use renewable energy.<sup>1,2</sup> Renewable energy utilization as an alternative of fossil fuels has a very positive impact in reducing greenhouse gas emissions and air pollution.<sup>3</sup>

The availability of solar energy at all times makes it a renewable energy source that is in great demand and is

used in various applications.<sup>4</sup> Solar energy has the advantage of being friendly to the environment and will not deplete over time compared with fossil natural resources. Consumption of fossil fuels impacts environmental pollution so many countries have switched to using renewable energy sourced from sunlight.<sup>3</sup>

Dye-sensitized solar cell (DSSC) is one of the latest innovations of photovoltaics that are economical, efficient, and environmentally friendly.<sup>5-7</sup> In general, DSSC consists of photoanode, sensitizer, the counter electrode (CE), and electrolyte pair ( $I^-/I_3^-$ ).<sup>5,8,9</sup> The working principle is based on light absorption by a dye and then

70 injecting electrons into the semiconductor's conduction band. Electrolytes are needed to generate dyes.<sup>1,6,10</sup>

Photoanode and sensitizer play an important role in increasing the efficiency of DSSCs. The most used photoanode material is titanium dioxide (TiO<sub>2</sub>). Its wide availability, harmlessness, good stability, and accessible synthesis make this oxide semiconductor material in great demand. The TiO<sub>2</sub>-based DSSC showed an efficiency of photoconversion of around 11%.<sup>59</sup> The addition of a dye sensitizer in the photoanode is essential for improving the performance of the DSSC.<sup>4,5</sup>

Dye sensitizers play a role in the direct absorption of sunlight and transfer electrons to the conduction band in semiconductor materials.<sup>2,3</sup> Ruthenium complex, metal-based dyes such as N3, N719, and N749 are chosen because of their high photovoltaic properties.<sup>3</sup> In 2020, Balachandran et al. used N3 dye, achieving an efficiency of 4.09%, and Kumar et al. used a different dye, N719, to achieve an efficiency of 6.34%.<sup>6</sup> Ruthenium dye (N3, N719) is a good chromophore in absorbing light, thereby increasing the efficiency of DSSC.<sup>4</sup>

Natural dyes are from fruits, vegetables, and plant parts, and both leaves and flowers have been used as photosensitizers in DSSC. Easy availability, inexpensive fabrication, and a friendly environment are the main points for selecting natural materials as photosensitizers.<sup>3,7,8</sup> Natural pigments derived from plants include carotenoids, chlorophyll, anthocyanins, and flavonoids. Carotenoids are in fruits and chlorophyll is found in leaves and flowers. Anthocyanins and flavonoids are also found in flowers.<sup>8</sup> Although natural dyes are used as photosensitizers, the efficiency values obtained are still low due to the limitations of its chemical structure and the aggregation formed on the surface of the photoanode.<sup>2,3</sup> This approach is for developing a new DSSC as guides in future from the narrative review of the previous published references especially on potential and relation between dye type and structural type in supporting efficiency. The review themes are structure types, DSSC working principle, and the dye sources (synthetic and natural). The influence of synthetic dyes and natural dyes on the physical properties, electronics, and efficiency of various DSSC structures and their fabrication methods are discussed and reported in detail.

## 44 2 | METHODS

### 2.1 | Search strategy and selection criteria

The research data were collected through searching various databases of www.scienceirect.com, MDPI (https://

www.mdpi.com/), and Research Gate. The latest research dominated in the last 3 years from the selected sources in the last 10 years. The search strategy includes a combination of terms and keywords "TiO<sub>2</sub>, DSSC (dye-sensitized solar cell), natural dye, synthetic dye, sandwich structure, monolithic structure, and honeycomb structure." The search is limited to the TiO<sub>2</sub> photoanodes with the addition of dye sensitizer and influence on the structure of DSSC. The initial stage is reading the suitability of the abstract, and then we conducted a very selective selection by considering all studies related to the TiO<sub>2</sub> photoanode, various dye sensitizers, and the structural pattern of the DSSC. The relevant abstracts were then observed further and discussed together by the authors. The results of further analysis are presented in Tables 1 to 3.

### 2.2 | Data analysis

Research data have gone through the selection stage that meets the author's observation review criteria, then information was collected related to the composition, type of dye, method, short-circuit current density ( $J_{sc}$ ), open-circuit voltage ( $V_{oc}$ ), fill factor (FF), energy conversion efficiency (ECE)/( $\eta$ ), and the type of DSSC structure. In particular, the effect of the type of dye sensitizer and DSSC structure on increasing photovoltaic efficiency is also discussed. There are three types of DSSC structures, namely, sandwich, monolithic, and honeycomb. The type of structure also plays an essential role in improving DSSC performance. The relationship between dye sensitizer and type of structure was observed and discussed together by the authors.

## 3 | DSSC STRUCTURE AND WORKING PRINCIPLES

DSSC generally consists of several interrelated components, while the DSSC components in question are as follows:

- The substrate commonly used is transparent conductive oxide (TCO). TCO has more than 80% efficiency and transparency, making it a good choice in DSSC manufacturing. There are two types of TCO used in the manufacture of DSSCs, namely fluorine tin oxide (FTO) and indium tin oxide (ITO). FTO has more stable conductivity and temperature resistance than ITO.<sup>8</sup>
- The morphology and bandgap of metal oxide semiconductor materials play an essential role in dye absorption and electron transfer. This metal oxide semiconductor serves as a photoanode in DSSC. The

**TABLE 1** Comparing DSSC performance parameters of synthetic dyes

References	Composition	Dye	Method	$J_{sc}$ ( $\text{mA}/\text{cm}^2$ )	$V_{oc}$ (V)	FF (%)	$\eta$ (%)
11	TiO <sub>2</sub> /ZnO	N719	RF-sputtered	16.63	0.727	59	7.1
12	TiO <sub>2</sub>		Co-sensitization	3.51	0.63	65.30	1.46
12	TiO <sub>2</sub> + W-NO <sub>2</sub>			6.12	0.59	71.11	2.60
13	TiO <sub>2</sub> :TiCl <sub>4</sub> treatment and Sr doping		Doctor blade	18.53	0.78	66	9.57
14	P25-TiO <sub>2</sub>		Sol-gel	14.2	0.755	66	6.4
14	TNPO-D (TiO <sub>2</sub> particles are prepared using dextran)			10.1	0.678	63	4.1
14	TNPO-G (TiO <sub>2</sub> particles are prepared using glucose)			8.9	0.673	63	3.7
15	Zn-doped TiO <sub>2</sub>			7.24	0.86	70	4.36
16	Zinc and gallium Co-doped TiO <sub>2</sub>			6.44	0.72	82	3.78
17	Cu-doped TiO <sub>2</sub>		Spin-coating	1.80	0.64	0.38	0.44
18	TiO <sub>2</sub>		Screen printing	19.63	0.72	54	7.41
18	TiO <sub>2</sub>		Spray coating	16.18	0.71	57	6.65
19	Nitrogen-doped TiO <sub>2</sub> /graphene nanofibers		Electrospinning and hydrothermal synthesis	15.38	0.71	46	5.01
20	TiO <sub>2</sub> + <i>O</i> -phenylenediamine capping TiO <sub>2</sub> with simple aromatic amines		Hydrothermal	18.4	0.763	70	80
21	1Cu/TiO <sub>2</sub>			7.34	1.073	65	5.09
21	2Mn/TiO <sub>2</sub>			7.87	1.119	49	4.32
22	TiO <sub>2</sub> and Pt + molybdenum diselenide (MoSe <sub>2</sub> )			11.2	0.66	40.11	2.967
23	TiO <sub>2</sub>			15.07	0.559	67.48	5.691
24	5 Fe-doped TiO <sub>2</sub>			8.37	0.939	0.35	2.74
24	5 Ni-doped TiO <sub>2</sub>	N719	Hydrothermal	7.75	1.126	0.51	4.47
24	5 Co-doped TiO <sub>2</sub>			6.87	1.201	0.59	4.85
24	Zn-doped TiO <sub>2</sub>			7.85	1.097	0.52	4.49
25	Hybrid TiO <sub>2</sub> /reduced graphene oxide (RGO)			20.6	0.79	53	8.62
26	TiO <sub>2</sub> nanoparticles (NPs), nanoleaves (NLs) only, and NLs + NPs			13.7	0.74	65	6.5
27	HMC-TiO <sub>2</sub>		Adopting the template method	16.1	0.808	68	8.77
28	TiO <sub>2</sub>		Doctor blade technique	20.1	0.71	0.54	7.71
12	TiO <sub>2</sub>	N719 + W-NO <sub>2</sub>	Co-sensitization	6.12	0.59	71.11	2.60
23	TiO <sub>2</sub>	N719 + N3	Co-sensitization	16.27	0.590	71.85	6.899
6	TiO <sub>2</sub>	N719 + CDA	Doctor blade technique	11.64	0.79	76	7.00
6	TiO <sub>2</sub>	RhB + CDA	Doctor blade technique	4.19	0.61	69	1.75
6	TiO <sub>2</sub>	D149 + CDA	Doctor blade technique	13.77	0.81	69	7.72

TABLE 1 (Continued)

References	Composition	Dye	Method	$J_{sc}$ (mA/cm <sup>2</sup> )	$V_{oc}$ (V)	FF (%)	$\eta$ (%)
4	10% Ag-TiO <sub>2</sub> :N3	N3	Sol-gel	258.0	0.468	46.6	5.60
29	TiO <sub>2</sub> /GO/Ag nanofiber	N3	Sol-gel	9.79	0.78	69.63	5.33
23	TiO <sub>2</sub>	N3	Co-sensitization	14.86	0.512	65.96	5.018
30	ZIF-8-RGO/TiO <sub>2</sub>	Indoline	Modified Hummers' method	17.8	0.679	60.6	7.33
30	Optimized UiO-66-RGO/TiO <sub>2</sub>	Indoline	Modified Hummers' method	18.6	0.678	60.8	7.67
21	1Cu/TiO <sub>2</sub>	Phen	Hydrothermal	1.50	0.790	51	0.61
21	1Mn/TiO <sub>2</sub>	Phen	Hydrothermal	1.33	0.849	51	0.58
21	1Cu/TiO <sub>2</sub>	Cu-Phen complex	Hydrothermal	2.18	1.298	52	1.47
21	1Mn/TiO <sub>2</sub>	Cu-Phen complex	Hydrothermal	2.36	1.296	46	1.41
21	1Cu/TiO <sub>2</sub>	Mn-Phen complex	Hydrothermal	3.20	1.115	57	2.03
21	1Mn/TiO <sub>2</sub>	Mn-Phen complex	Hydrothermal	4.87	0.881	46	1.98
21	1Cu/TiO <sub>2</sub>	Cr-Phen complex	Hydrothermal	2.94	1.166	48	1.65
21	1Mn/TiO <sub>2</sub>	Cr-Phen complex	Hydrothermal	4.60	0.792	43	1.58
5	TiO <sub>2</sub>	The Eosin Blue dye	Doctor blade technique	10.98	0.4554	45.98	2.30

Abbreviations: DSSC, dye-sensitized solar cell; FF, fill factor.

large surface area will increase the absorption of dyes so that light absorption will be more optimal.<sup>1,3</sup>

- The dye is a part of a photosensitizer for producing current, which adheres to metal oxide semiconductors through covalent bonds.<sup>1</sup> An effective photosensitizer will provide high absorption. Photosensitizers are three parts: metallic, nonmetallic, and natural organic dyes.<sup>8,9</sup>
- Commonly used electrolytes are from iodine/triiodide ( $I^-/I_3^-$ ) redox couple dissolved in a suitable solvent, usually acetonitrile, and some additional additives to improve cell performance. Electrolytes are needed to regenerate dyes and to complete electron transport at the electrodes.<sup>1,10</sup>
- CE is generally made of platinum (Pt) catalyst. A thin layer of platinum is deposited on the TCO glass. CE plays a role in the reduction of triiodide resulting from the regeneration of dyes into iodide ions.<sup>1,10</sup>

In general, the structures of DSSC are sandwich structure, monolithic structure, and honeycomb structure.

### 3.1 | Sandwich structure

The schematic representation of the DSSC for the sandwich structure is presented in Figure 1A, which consists of three main components: photoanode, dye-sensitized electrolyte, and conductive CE.<sup>7</sup>

For the photoexcitation process, the dye releases excited electrons and transfers them to the semiconductor layer's conduction band (TiO<sub>2</sub>).<sup>65</sup> The electrons will be adsorbed by TiO<sub>2</sub> and collected on a glass substrate with TCO. The electrons then pass through the external circuit to the CE. Furthermore, the process of reducing triiodide ions ( $I_3^-$ ) to iodide ions ( $I^-$ ) occurs at the CE.<sup>66</sup> Iodide generates from reduction triiodide by the electrons at the external circuit, which can easily be understood by using the following equations<sup>65,67</sup>:

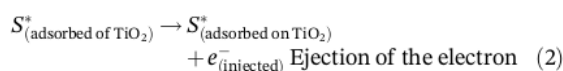


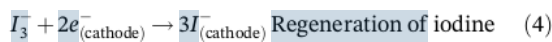
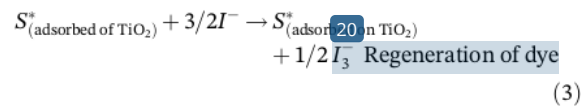
TABLE 2 Comparing DSSC performance parameters of natural dyes

References	Composition	Dye	Method	$J_{sc}$ (mA/cm <sup>2</sup> )	$V_{oc}$ (V)	FF (%)	$\eta$ (%)
31	TiO <sub>2</sub>	Beet root	Hydrothermal	4.38	1.623	0.60	14.21
32		The black mulberry	Doctor blade	0.463	0.374	0.373	5.10
33		<i>Acalypha amantacea</i> + <i>Peltophorum pterocarpum</i>	Sol-gel	14.95	0.834	65.87	8.22
34		<i>Hybrid agaricus bisporus</i> : <i>Citrus limonum</i> leaves extract	Doctor blade	1.91	0.489	0.578	0.54
35		<i>Punica granatum</i> (Pomegranate)	Electrophoretic deposition (EPD)	0.40	0.62	0.61	0.15
36			Simple and green successive ionic layer adsorption and reaction	1.62	0.304	0.209	0.20
37			Photosynthesis process	1.57	0.480	36	1.12
38			Doctor blade	4.5	0.32	0.70	1,008
38		<i>Malus domestica</i> (Apple)		4.48	0.32	0.59	0.85
38		<i>Raphanus sativus</i> (Red radish)		3.12	0.33	0.71	0.73
38		<i>Solanum melongena</i> (Egg plant)		4.51	0.33	0.74	1.10
38		<i>Phoenix dactylifera</i> (Date)		4.21	0.33	0.58	0.81
39		<i>Elaeagnus conferta</i>	Solid state	6.00	0.49	0.87	2.50
37		<i>Melastoma malabathricum</i>	Photosynthesis process	0.88	0.380	43	0.76
40	Na + Yeast-TiO <sub>2</sub>	<i>Hibiscus sabdariffa</i> (Roselle)	Hydrothermal	6.9	0.62	0.561	2.40
41	Sodium (Na)-doped titanium dioxide (TiO <sub>2</sub> ) nanorods	<i>H sabdariffa</i> (Roselle)		5.5	0.55	0.545	1.65
42	Na-doped TiO <sub>2</sub>	<i>H sabdariffa</i> (Roselle)		6.0	0.54	0.481	1.56
43	TiO <sub>2</sub>	<i>Calliandra haematocephala</i>	TiO <sub>2</sub> thin film based dye-sensitized	0.25	0.370	70	0.06
43	TiO <sub>2</sub>	<i>P pterocarpum</i>	TiO <sub>2</sub> thin film based dye-sensitized	0.15	0.400	71	0.04
33	TiO <sub>2</sub>	<i>P pterocarpum</i>	Sol-gel method	13.22	0.871	62.22	7.17
28	TiO <sub>2</sub>	<i>Chrysanthemum</i>	Doctor blade	20.1	0.71	0.54	7.71
44	TiO <sub>2</sub>	Purple daisy flowers	Spin-coating	0.181	0.42	0.168	0.197
44	TiO <sub>2</sub>	Yellow daisy flowers	Spin-coating	0.185	0.52	0.210	0.304
44	TiO <sub>2</sub>	Wine daisy flowers	Spin-coating	0.387	0.52	0.262	0.792
35	TiO <sub>2</sub>	<i>Reseda luteola</i>	EPD	0.54	0.64	63.60	0.22
35	TiO <sub>2</sub>	<i>Berberis integerrima</i>	EPD	0.004	0.56	0.53	0.01
35	TiO <sub>2</sub>	<i>Panica granatum pleniflora</i>	EPD	0.40	0.62	0.61	0.15

TABLE 2 (Continued)

References	Composition	Dye	Method	$J_{sc}$ (mA/cm <sup>2</sup> )	$V_{oc}$ (V)	FF (%)	$\eta$ (%)
35	TiO <sub>2</sub>	<i>Consolida orientalis</i>	EPD	0.56	0.60	0.53	0.18
35	TiO <sub>2</sub>	<i>Reseda gredensis</i>	EPD	0.14	0.53	0.71	0.07
35	TiO <sub>2</sub>	<i>Consolida ajacis</i>	EPD	1.68	0.55	0.65	0.60
35	TiO <sub>2</sub>	<i>Adonis flammea</i>	EPD	0.40	0.59	0.66	0.16
35	TiO <sub>2</sub>	<i>Salvia sclarea</i>	EPD	0.10	0.37	0.54	0.02
35	TiO <sub>2</sub>	<i>Clematis orientalis</i>	EPD	0.22	0.42	0.49	0.05
7	TiO <sub>2</sub>	<i>Thunbergia erecta</i>	Spin coating	0.27	0.55	0.40	0.37
45	TiO <sub>2</sub>	<i>Iris persica</i> (Lily)	Electrospinning	2.716	0.738	86	1.720
37	TiO <sub>2</sub>	<i>Begonia malabarica</i> Lam. (BM)	Photosynthesis process	2.15	0.500	35	1.76
46	Zirconium oxide post treated tin doped TiO <sub>2</sub>	Leaves of <i>Camellia sinensis</i> (green tea)	Sol-gel and hydrothermal	5.21	0.747	53.4	2.09
33	TiO <sub>2</sub>	<i>A amantacea</i>	Sol-gel method	11.45	0.747	59.48	5.08
47	TiO <sub>2</sub> -dye/ITO	<i>Pterocarpus indicus</i> Willd (leaf extract)	A slip casting	0.137	0.415	0.406	0.023

Abbreviations: DSSC, dye-sensitized solar cell; FF, fill factor; RGO, reduced graphene oxide.



The external load applied provided by the light works in the photovoltaic energy conversion system, which can regenerate and stabilize.<sup>65</sup>

### 3.2 | Monolithic structure

The monolithic structure can be clearly distinguished from the sandwich structure by the shape and composition of the material.<sup>64</sup> The sandwich structure consists of two glass plates coated with FTO. In contrast, the monolithic structure consists of only one FTO-coated glass plate, so that the manufacturing cost is relatively cheaper than the sandwich structure.<sup>68</sup>

Solar cells with a monolithic structure use composite layers as CE. All cells are grown on a single substrate; this distinguishes between monolithic structures and sandwich structures. In a monolithic structure, the CE is above the photoelectrode (PE). PE is grown by deposition of TiO<sub>2</sub>, followed by printing a porous insulating spacer layer (usually consisting of ZrO<sub>2</sub>) on the top. This porous layer serves as an intermediary between PE and CE.<sup>64,69</sup> The

material used as the spacer layer must be transparent. To make the layer transparent in a monolithic structure, the refractive index of the spacer layer must be close to the refractive index of the electrolyte used in the DSSC.<sup>70</sup>

PEs absorb light and produce photons. The tethering of the dye molecules will result in more light absorption so that more photon current is generated. The catalyst (must be conductive) plays a role in diffusing the charge carrier into the liquid electrolyte. The catalyst layer generally consists of a thick layer of porous carbon. The carbon layer is the only conductor layer in CE and must have sufficient sheet resistance.<sup>64,71</sup>

Liquid redox electrolyte serves as a carrier hole and regenerates the dye molecules, increasing photocurrent value. Thermoplastic polymer located between photoanode and CE was used for sealing device to avoid leakage of liquid electrolyte.<sup>71</sup>

DSSCs with monolithic structures generally show lower efficiencies than sandwich structures due to the ability for isolation and block diffusion of ion. Carefully selecting electrolytes in preparation of this structure is very crucial. Inappropriate electrolytes can damage the retaining layer of the TCO. Therefore, a nonvolatile solvent is needed to avoid leakage.<sup>64</sup>

### 3.3 | Honeycomb structure

The honeycomb structure has a structure more or less the same as the conventional structure consisting of PE,

TABLE 3 Three types of DSSC structures are sandwich, monolithic, and honeycomb structures

Photoanode	Structure	Remarks	References
TiO <sub>2</sub>	Sandwich	TiO <sub>2</sub> with organic dye-RhB, D149, and N719 + 10 mM CDA (chenodeoxycholic acid)	6
		A hybrid blend of natural dyes <i>Agaricus bisporus</i> (Mushroom) and <i>Citrus limonum</i> (Lemon) leaves as a photosensitizer	34
Cu-doped TiO <sub>2</sub>		Two-dimensional nanowall of Cu-doped TiO <sub>2</sub> as photoanode in a DSSC	17
Nitrogen-graphene co-doped TiO <sub>2</sub>		Nitrogen and graphene co-doped TiO <sub>2</sub> were prepared using the doctor blade method.	19
TiO <sub>2</sub>		Metals (Cu, Mn, Cr, and Phen complex) are used to doping TiO <sub>2</sub> using the hydrothermal method	21
HMC-TiO <sub>2</sub>		The composite HMC (highly mesoporous carbons)-TiO <sub>2</sub>	27
Metal-organic frameworks (MOFs)-ZIF-8/TiO <sub>2</sub>		MOFs-ZIF-8 and reduced graphene oxide (RGO) as photoanodes	30
MOFs-Uio-66/TiO <sub>2</sub>		MOFs-Uio-66 and RGO as photoanodes	30
TiO <sub>2</sub>		TiO <sub>2</sub> with natural dye-black mulberry ( <i>Morus nigra</i> ) and gel electrolytes	32
		TiO <sub>2</sub> with natural dye (anthocyanin) extracted from pomegranate fruit	36
		TiO <sub>2</sub> with natural dyes containing luteolin extracted from daisy flowers	44
TiO <sub>2</sub> -dye/ITO		The chlorophyll content of <i>Pterocarpus indicus</i> Willd leaves as a sensitizer for DSSC applications	47
La <sub>2</sub> O <sub>3</sub> /TiO <sub>2</sub>	Monolithic	In this study, photocatalytic activity of La-loaded TiO <sub>2</sub> NFs was enhanced by engineering approach using monolithic honeycomb-assisted photoreactor system for dynamic hydrogen production	48
TiO <sub>2</sub> /PET	Monolithic	TiO <sub>2</sub> films supported on polyethylene terephthalate (TiO <sub>2</sub> /PET) in sheets and monolithic shapes were prepared from reused PET bottles	49
ITO/TiO <sub>2</sub> interface and TiO <sub>2</sub> layer	Monolithic	Low-temperature perovskite solar cells with an evaporated TiO <sub>2</sub> compact layer for perovskite silicon tandem solar cells	50
Cr(VI) over TiO <sub>2</sub> -coated cellulose acetate	Monolithic	Photocatalytic reduction of Cr(VI) over TiO <sub>2</sub> -coated cellulose acetate monolithic structures using solar light	51
Silver-modified TiO <sub>2</sub>	Monolithic	Photo-induced CO <sub>2</sub> reduction by hydrogen for selective CO evolution in a dynamic monolith photoreactor loaded with Ag-modified TiO <sub>2</sub> nanocatalyst	52
Au/TiO <sub>2</sub>	Monolithic	Synergistic effect in MMT-dispersed Au/TiO <sub>2</sub> monolithic nanocatalyst for plasmon absorption and metallic interband transitions dynamic CO <sub>2</sub> photoreduction to CO	53
Lanthanum and nitrogen—co-doped SrTiO <sub>3</sub> —TiO <sub>2</sub>	Monolithic	Fabrication of lanthanum and nitrogen—co-doped SrTiO <sub>3</sub> —TiO <sub>2</sub> heterostructured macroporous monolithic materials for photocatalytic degradation of organic dyes under visible light	54
TiO <sub>2</sub>	Monolithic	High surface area stainless steel wire mesh-supported TiO <sub>2</sub> prepared by sacrificial template accelerated hydrolysis. A monolithic photocatalyst superior to P25 TiO <sub>2</sub>	55
TiO <sub>2</sub>	Monolithic	Hybrid energy storage devices based on monolithic electrodes containing well-defined TiO <sub>2</sub> nanotube size gradients	56

TABLE 3 (Continued)

Photoanode	Structure	Remarks	References
Rh/TiO <sub>2</sub> -sepiolite	Monolithic	Development of a new Rh/TiO <sub>2</sub> -sepiolite monolithic catalyst for N <sub>2</sub> O decomposition	57
TiO <sub>2</sub>	Honeycomb	This work optimized the combined anti-reflection and scattering properties of two types of light trapping (LT) structures, based on TiO <sub>2</sub> semispheroidal geometries with honeycomb periodicity	36, 14, 58
TiO <sub>2</sub> nanotubes (NTs)	Honeycomb	Fabrication of TiO <sub>2</sub> -NTs and TiO <sub>2</sub> -NTs covered honeycomb lattice and investigation of carrier densities in I/13 electrolyte by electrochemical impedance spectroscopy	2, 59
Boron and nitrogen co-doped TiO <sub>2</sub>	Honeycomb	Highly textured boron/nitrogen co-doped TiO <sub>2</sub> with honeycomb structure showing enhanced visible-light photoelectrocatalytic activity	7, 60
Anatase TiO <sub>2</sub>	Honeycomb	Seeding-method-processed anatase TiO <sub>2</sub> film at low temperature for efficient planar perovskite solar cell	8, 61
Three-dimensional ordered macroporous (3DOM) TiO <sub>2</sub>	Honeycomb	Novel precursor-reforming strategy to the conversion of honeycomb-like 3DOM TiO <sub>2</sub> to ant nest-like macro-mesoporous N-TiO <sub>2</sub> for efficient hydrogen production	1, 62
TiO <sub>2</sub> nanotube	Honeycomb	Honey-combed TiO <sub>2</sub> nanotube arrays with top-porous/bottom—tubular structures for enhanced photocatalytic activity	1, 63
rGO-TiO <sub>2</sub> nanocomposite	Honeycomb	Effect of co-sensitization in solar exfoliated TiO <sub>2</sub> -functionalized rGO photoanode for dye-sensitized solar cell applications	6, 23
TiO <sub>2</sub>	Monolithic	Carbon film-based monolithic perovskite solar cells were made using TiO <sub>2</sub> nanoparticles as a binder	69, 48
TiO <sub>2</sub> , ZrO <sub>2</sub> , Al <sub>2</sub> O <sub>3</sub>		Carbon-based perovskite solar cells with various mesoporous structures TiO <sub>2</sub> + Al <sub>2</sub> O <sub>3</sub> TiO <sub>2</sub> + ZrO <sub>2</sub> , Al <sub>2</sub> O <sub>3</sub> , TiO <sub>2</sub>	35, 49
ITO/TiO <sub>2</sub> interface and TiO <sub>2</sub> layer		Perovskite solar cells with low temperature treatment on the device monolithic tandem	66, 50
TiO <sub>2</sub> + ZrO <sub>2</sub>		The thickness of the layer between the photoanode and the electrode in a monolithic DSSC affects the lifetime of the electron. The porous layer was chosen because it has the ability to reduce charge transfer resistance	51
TiO <sub>2</sub>		Optical simulation of DSSC with perovskite monolithic structure in analyzing the potential for increasing efficiency of DSSC devices	52
TiO <sub>2</sub>		Development of the blocking layer-transfer skeleton structure with two-step hydrothermal synthesis to improve the injection and charge transfer capabilities of DSSC	53
Nb-doped TiO <sub>2</sub>		Electrical conductivity of TiO <sub>2</sub> -doped Nb deposited on p-type Si substrates	54
TiO <sub>2</sub> and ZrO <sub>2</sub>		Perovskite solar cells based on carbon counter electrodes (TiO <sub>2</sub> and ZrO <sub>2</sub> ) are made without hole-transporting materials (HTM) to improve device performance	55
TiO <sub>2</sub>		A bipolar electrochemical approach is used to make TiO <sub>2</sub> thin films that can be applied as energy storage	56

(Continues)

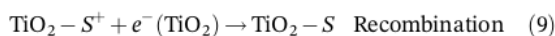
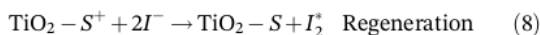
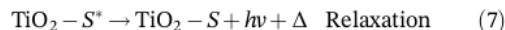
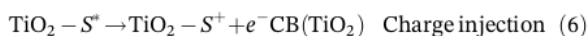
TABLE 3 (Continued)

Photoanode	Structure	Remarks	References
TiO <sub>2</sub> -In <sub>2</sub> O <sub>3</sub>		Perovskite solar cells are made with TiO <sub>2</sub> -In <sub>2</sub> O <sub>3</sub> photoanode as an electron transport layer. TiO <sub>2</sub> -In <sub>2</sub> O <sub>3</sub> is effective in reducing the rate of electron recombination thereby improving device performance	57
TiO <sub>2</sub>	Honeycomb	The application of perovskite solar cells is optimized by combining the anti-reflection and scattering properties of light trapping	58
TiO <sub>2</sub> nanotubes (NTs)	Honeycomb	Fabrication of TiO <sub>2</sub> -NTs and TiO <sub>2</sub> -NTs covered honeycomb lattice and investigation of carrier densities in I/13 electrolyte by electrochemical impedance spectroscopy	59
Boron and nitrogen co-doped TiO <sub>2</sub>	Honeycomb	Highly textured boron/nitrogen co-doped TiO <sub>2</sub> with honeycomb structure showing enhanced visible-light photoelectrocatalytic activity	60
Anatase TiO <sub>2</sub>	Honeycomb	Seeding-method-processed anatase TiO <sub>2</sub> film at low temperature for efficient planar perovskite solar cell	61
3DOM TiO <sub>2</sub>	Honeycomb	Novel precursor-reforming strategy for the conversion of honeycomb-like 3DOM TiO <sub>2</sub> to ant nest-like macro-mesoporous N-TiO <sub>2</sub> for efficient hydrogen production	62
TiO <sub>2</sub> nanotube	Honeycomb	Honey-combed TiO <sub>2</sub> nanotube arrays with top-porous/bottom—tubular structures for enhanced photocatalytic activity	63
rGO-TiO <sub>2</sub> nanocomposite	Honeycomb	Effect of co-sensitization in solar exfoliated TiO <sub>2</sub> functionalized rGO photoanode for dye-sensitized solar cell applications	23
TiO <sub>2</sub>	Honeycomb	The application of perovskite solar cells is optimized by combining the antireflection and scattering properties of light trapping	58
TiO <sub>2</sub> nanotube		Honeycomb TiO <sub>2</sub> nanotubes were prepared using a two-step anodization method	63
rGO-TiO <sub>2</sub> nanocomposite		Nanocomposites (rGO-TiO <sub>2</sub> ) were prepared using the hydrothermal method for DSSC photoanode applications	23
TiO <sub>2</sub> nanotubes (NTs)		TiO <sub>2</sub> nanotubes, prepared by a two-stage anodization technique, are effective in photoanode applications	59
Boron and nitrogen co-doped TiO <sub>2</sub>		TiO <sub>2</sub> photocatalyst prepared by the oxidation process and doping (boron and nitrogen) simultaneously with a honeycomb structure	60
TiO <sub>2</sub>		Anatase TiO <sub>2</sub> was prepared by seeding method at low temperatures for perovskite solar cell applications	61
3DOM TiO <sub>2</sub>		The photocatalytic activity of nitrogen-doped TiO <sub>2</sub> is enhanced based on the 3DOM structure	62

glass substrate and TCO as a conducting layer, a CE made of platinum (Pt) coated on the TCO surface, a sensitized dye, and an electrolyte solution inserted between the two electrodes.<sup>72</sup> The difference is for CE, where the hexagonal structure is like a honeycomb.<sup>1,73</sup>

Platinum is commonly used for CE in the manufacture of DSSCs, but platinum is replaced by graphene for the honeycomb structure. Graphene is a carbon nanotube material, which has  $sp^2$  bonds packaged in a honeycomb-like crystal lattice.<sup>74</sup> Graphene has excellent electrical and optical properties.<sup>75</sup> This structure shows a much higher conversion efficiency than conventional DSSCs.<sup>73</sup>

The working principle of the honeycomb structure is similar to a sandwich or conventional structure where the dye layer absorbs light, and then the excited dye will release electrons. Those electrons will jump to the conduction band of the semiconducting layer ( $TiO_2$ ).<sup>65</sup> The electrons will be adsorbed by  $TiO_2$  and collected on a glass substrate with a TCO. The electrons then pass through the external circuit to the CE. Furthermore, the process of reducing triiodide ions ( $I_3^-$ ) to iodide ions ( $I^-$ ) occurs at the CE.<sup>66</sup> The iodide is regenerated by triiodide reduction by utilizing electrons from the external circuit,<sup>65,67</sup> which are presented in the following chemical reactions for convenience<sup>72</sup>:



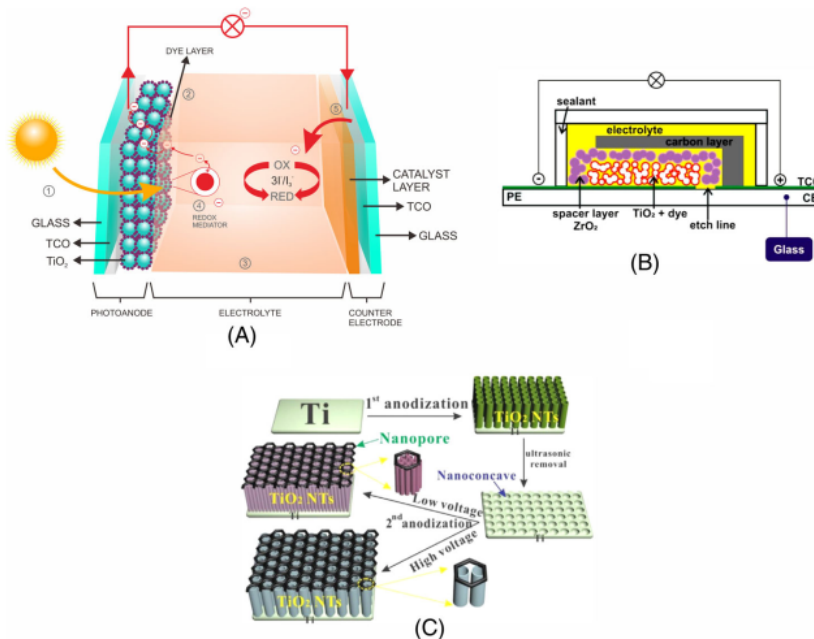
### 3.4 | DSSC photovoltaic performance

DSSC performance can be identified by four photovoltaic parameters:  $J_{sc}$ ,  $V_{oc}$ , FF, and  $(ECE)/(\eta)$ .<sup>67</sup>

The cell absorbs sunlight and then various values of voltage is applied to produce an electric current. The formed photocurrent density–voltage ( $J - V$ ) curve is used from the lighting process to determine the maximum power of cell fabrication. The plot results between the current and voltage curves are used to analyze the photovoltaic performance. DSSC FF and conversion efficiency are determined by using the following equations<sup>4,24</sup>:

$$FF = \frac{V_{max} \times J_{max}}{V_{oc} \times J_{sc}} \quad (11)$$

$$\eta = \frac{FF \times V_{oc} \times J_{sc}}{P_{in}} \times 100\% \quad (12)$$



50 FIGURE 1 Various structures in the DSSC fabrication. (A) Sandwich,<sup>64</sup> (B) monolithic,<sup>64</sup> and (C) honeycomb<sup>63</sup>

The  $P_{in}$  is power input (1000 W/cm<sup>2</sup>). Efficiency ( $\eta$ ) depends on the value of  $V_{oc}$  and  $J_{sc}$  and can be seen in Equation (12). If the input power is constant, the efficiency value will also increase by increasing the value of  $V_{oc}$  and  $J_{sc}$ .<sup>76,77</sup>

$J_{sc}$  indicates the number of photocurrent during the irradiation process and high correlation to the number of absorbed photons by the dye per unit area.  $J_{sc}$  depends on the coefficient of the dye sensitizer at the photoanode (TiO<sub>2</sub>).  $J_{sc}$  can be defined by using the equation<sup>76,77</sup>:

$$J_{sc} = \int_{\lambda} \text{LHE}(\lambda) \phi_{\text{inject}} \eta_{\text{collect}} d\lambda \quad (13)$$

LHE( $\lambda$ ) denotes the light harvesting at the maximum wavelength, and the electron injection efficiency is denoted by  $\phi_{\text{inject}}$ . The charge collection efficiency is constant and independent of the type of sensitizer denoted by  $\eta_{\text{collect}}$  and the LHE( $\lambda$ ) equation is as follows<sup>76,77</sup>:

$$\text{LHE}(\lambda) = 1 - 10^{-f}, \quad (14)$$

where  $\lambda$  is the given wavelength and  $f$  is the oscillatory strength of the dye molecule. Furthermore,  $\phi_{\text{inject}}$  corresponds to the driving force of  $\Delta G^{\text{inject}}$  for the electron injection through the linkage between semiconductor layer and the dye, which is explained using the following equation<sup>76</sup>:

$$\phi_{\text{inject}} \propto f(-\Delta G^{\text{inject}}), \quad (15)$$

so  $\Delta G^{\text{inject}}$  can be written as

$$\Delta G^{\text{inject}} = E^{\text{dye}*} - E_{CB}, \quad (16)$$

where  $E^{\text{dye}*}$  is the energy oxidation potential of the excited dye and  $E_{CB}$  is the ground state reduction potential of the conduction band semiconductor (TiO<sub>2</sub>) ( $E_{CB}(\text{TiO}_2) = -4.0 \text{ eV}$ ).<sup>76</sup>

For evaluating the DSSC performance, the regeneration efficiency of the dye is also essential to observe through the regeneration driving force of  $\Delta G_{\text{reg}}$ . It is calculated from the difference between the ground state and oxidation potential<sup>77</sup>:

$$\Delta G_{\text{reg}} = E_{I^-/I_3^-} - E_{\text{dye}}. \quad (17)$$

Another factor that affects to the efficiency is  $V_{oc}$ , which determined by using the equation<sup>77</sup>:

$$V_{oc} = \frac{E_{CB} + \Delta E_{CB}}{q} + \frac{k_B T}{q} \ln \left( \frac{n_c}{N_{CB}} \right) - \frac{E_{\text{redox}}}{q}, \quad (18)$$

where the charge is denoted by  $q$ , the Boltzmann constant is  $k_B$ , the edge of the conduction band is  $E_{CB}$ , and the absolute temperature is  $T_s$ . At the conduction band, the number of electrons is denoted by  $n_c$ , while the density is denoted by  $N_{CB}$  and the Fermi level of the electrolyte is denoted by  $E_{\text{redox}}$ . If the dye is adsorbed on the surface of TiO<sub>2</sub>, there is a shift in  $\Delta E_{CB}$  as shown in the following equation<sup>77</sup>:

$$\Delta E_{CB} = -\frac{q\mu_{\text{normal}}\gamma}{\epsilon_0} \epsilon. \quad (19)$$

The dipole moment of the sensitizer perpendicular to the surface of the semiconductor (TiO<sub>2</sub>) is denoted by  $\mu_{\text{normal}}$ , the surface concentration of the dye is  $\gamma$ . The dipole layer representing vacuum and electric permittivity is  $\epsilon_0$  and  $\epsilon$ , respectively. If increase in  $\mu_{\text{normal}}$  will affect in enlarging the shift of  $\Delta E_{CB}$ , consequently the value of  $V_{oc}$  also increases.<sup>77</sup>

## 4 | DYES AS PHOTSENSITIZERS

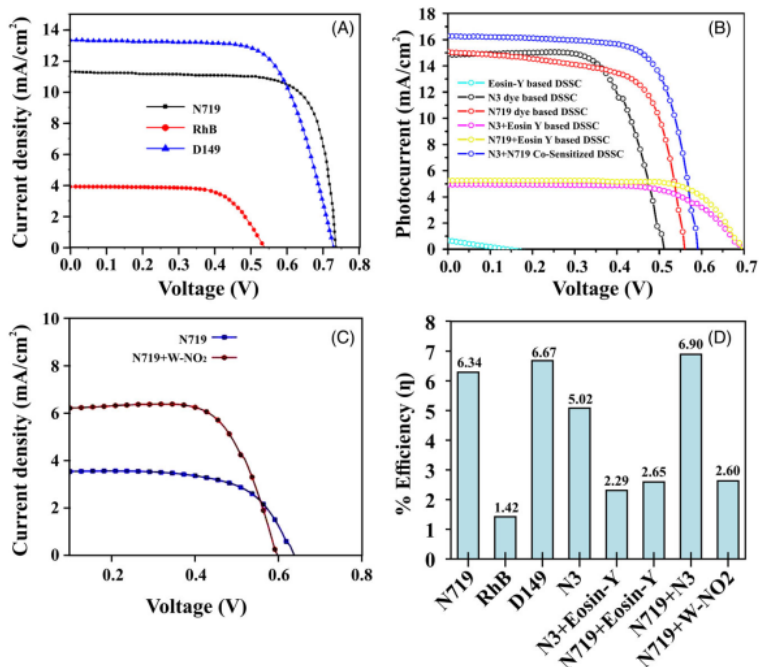
### 4.1 | Synthetic dye

The addition of a single synthetic dye or combination of several natural dyes has quite an effect on improving DSSC performance.<sup>23</sup> Dye absorption and film resistance are related to photon flow. If the number of dye molecules on the PE immediately increases, the light absorption efficiency<sup>51</sup> also increases. This phenomenon can be determined by the density-voltage.<sup>78</sup>

The  $J-V$  characteristic curves of TiO<sub>2</sub> PEs with various types of dye synthetics are shown in Figure 2A-C. The  $J-V$  characteristic curves used to determine the photovoltaic characteristics of the DSSC are  $J_{sc}$ ,  $V_{oc}$ , FF, and  $\eta$ .<sup>79</sup> Photovoltaic characteristics of various journal references are shown in Table 1. Photoanodes sensitized with organic dyes N719, RhB, and D149 showed photoconversion efficiencies of 6.34%,<sup>38</sup> 1.42%, and 6.67%, respectively.<sup>6</sup> Observations made using a combination of metal-free and metal-based organic dyes, namely N3, N3 + Eosin-Y, N719 + Eosin Y, N719 + W-NO<sub>2</sub>, and N719 + N3, showed significant results obtained by efficiency values of 5.02%, 2.29%, 2.65%, 2.60%, and 6.90% respectively.<sup>12,23</sup> Combining two dyes can increase the efficiency value of the material.

The combination of two complex metal dyes showed a better efficiency increase than metal and nonmetal

**FIGURE 2** <sup>10</sup> Current-voltage curves of DSSCs sensitized with (A) RhB, D149, and N719, <sup>6</sup> (B) Eosin-Y, N3, N719, N3 + Eosin-Y, N719 + Eosin Y, and N719 + N3, <sup>23</sup> (C) N719, N719 + W-NO<sub>2</sub>, <sup>12</sup> (D) comparison of photoconversion efficiency from graphs (A) to (C)



dyes. This increase is associated with the value of  $J_{sc}$ . The increase in  $J_{sc}$  in the 350 to 400 nm of the solar spectrum lead to an increase in photons, thus indicated by an increase in the extinction coefficient and absorption region.<sup>12</sup> The comparison of the photoconversion efficiency value is shown in Figure 2D.

## 4.2 | Natural dye

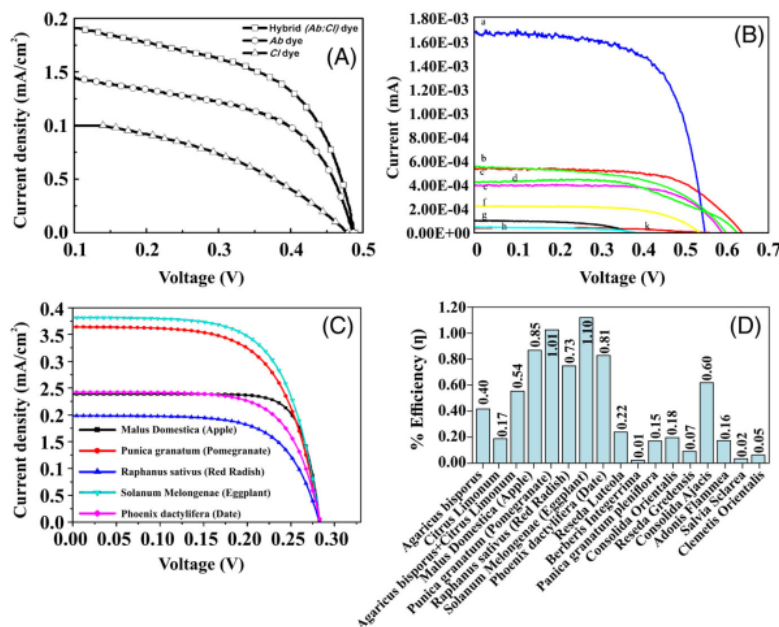
<sup>28</sup> The  $J-V$  curve of the TiO<sub>2</sub> PF<sub>6</sub> with various natural dyes is shown in Figure 3A-C.  $J_{sc}$ ,  $V_{oc}$ , FF, and  $\eta$  are obtained from the  $J-V$  curve where the corresponding results are given in Table 2. The photoconversion efficiency of various natural dyes is shown in Figure 3D. The efficiency of natural sensitizers extracted from mushrooms was obtained by an efficiency value of 0.40%, while for the types of plants (flowers, leaves, roots) the efficiency values ranged from 0.01% to 0.50%. Based on the characteristic photovoltaics, the natural dyes extracted from plants have a higher photocurrent and ECE than natural dye extracts. These may be due to broader absorption of sunlight and availability of the natural pigment Delphinidin (a type of anthocyanin).<sup>35</sup>

The Pervez study in 2018 used fruit and vegetable extracts as dye sensitizers for DSSC.<sup>38</sup> Efficiency graph in Figure 3D shows the efficiency value of fruit ranging from 0.17% to 1.10%, while that of vegetables is 0.73%. The better performance of DSSC is due to the molecular

structure of riboflavin and chlorophyll pigment. Chlorophyll is used as a sensitizer for the manufacture of DSSCs,<sup>80</sup> where the ability to absorb solar energy by chlorophyll molecules promotes higher electron transfer performance.<sup>34</sup>

## 4.3 | Synthetic dyes in DSSC application

By increasing the efficiency of DSSC, one of the essential factors is the absorption spectrum of the photosensitizer dye. Dye represents the core component of DSSC and has the function of receiving photons and also anode sensitization.<sup>7</sup> Zatirostami<sup>11</sup> in his journal used N719 dye to improve its photovoltaic performance and applied a blocking layer at the interface TiO<sub>2</sub>/ZnO for reduce recombination problems. In his research, he found an increase in DSSC efficiency by 7.1%. The efficiency of co-sensitization of WNO<sub>2</sub> dye with N719 sensitizer obtained a significant increase compared with individual N719 dye, that is, 2.60%.<sup>12</sup> With the same method, co-sensitization,<sup>23</sup> the combination of complex metal-based dyes showed better efficiency results with an efficiency of 6.899%,<sup>6</sup> synthesized TiO<sub>2</sub> photoanodes with various kinds of organic dyes, namely N719, RhB, and D149. By addition of CDA in the dye solution, the DSSC performance increase with the efficiency values for N719, RhB, and D149 is 7.00%, 1.75%, and 7.72%, respectively.



52  
28  
FIGURE 3 Current-voltage curves of DSSCs sensitized with natural dye extracts of (A) mushroom and lemon leaves,<sup>34</sup> (B) fruits and vegetables,<sup>38</sup> (C) plants,<sup>35</sup> and (D) comparison of photoconversion efficiency from graphs (A) to (C)

DSSCs based on Ag-TiO<sub>2</sub> film with the addition of N3 dye showed better photovoltaic performance than ordinary TiO<sub>2</sub> films. The absorption of N3 dye enhances by the presence of Ag doping, which expands the surface area of the TiO<sub>2</sub> film. The increase in N3 dye is related to the electronic absorption spectrum, thereby improving the light-harvesting properties.<sup>4</sup> et al<sup>30</sup> investigated the metal-organic framework and reduced graphene oxide (RGO) use to modify the DSSCs for enhancing photovoltaics. With the addition of Indoline dye, the photovoltaic performance of DSSC obtained an efficiency increase to 7.67%.

Unlu and Ozacar<sup>21</sup> synthesized TiO<sub>2</sub> photoanodes with various dyes (N719, Phen, Cu-Phen complex, Mn-Phen complex, Cr-Phen complex) doped Cu and Mn to improve photovoltaic performance. The process of recombination and electron transfer is affected by the amount of dopant and dye sensitizer. Cu doping obtained a better efficiency value with the addition of dye sensitizing the Mn-Phen complex. There is a strong electrostatic interaction between Cu ions and dye molecules, thereby reducing the agglomeration rate and increasing the electron injection and ECE of DSSC. In another study, Raguram<sup>5</sup> used synthetic organic dye (Eosin Blue [EB]) with an efficiency of 2.30%.

#### 4.4 | Natural dyes in DSSC application

Natural dyes are environmentally friendly and easy to extract, so they are suitable as sensitizers for DSSCs.<sup>81</sup>

Various types of natural dyes have been reported such as fruits, vegetables, and plants. As Desai has done,<sup>31</sup> a thin layer of TiO<sub>2</sub> was added with a dye betanin from beetroot with various concentrations in his research. DSSC performance increased from 5.82% to 14.21% along with the increase in deposition time.

An efficiency value of 0.54% was obtained for the efficiency of natural sensitizers extracted from mushrooms + *Citrus limonum* leaves. For the types of plants (flowers, leaves, roots), the efficiency values ranged from 0.01% to 7.71%. The improved ECE is due to the natural pigment Delphinidin (a type of anthocyanin) contained in the dye.<sup>35</sup> The efficiency value of fruit ranges from 0.17% to 1.10%, while that of vegetables is 0.73%. The better performance of DSSC is due to the molecular structure of riboflavin and chlorophyll pigment,<sup>80</sup> where the ability to absorb solar energy by chlorophyll molecules promotes higher electron transfer performance.<sup>34</sup>

In addition to the coloring factor, the composition of the constituent materials is also essential. Doping has a significant effect in increasing the surface area,<sup>40-42</sup> which allows the absorption of more sunlight so that ECE increases.<sup>35</sup>

#### 4.5 | DSSC structure

The schematic representation of the DSSC for sandwich structures is generally composed of three main components, namely photoanode, electrolytes with redox pairs, and CEs. Arrange the structure in an orderly manner in a sandwich layer so that it is called a sandwich structure.<sup>7</sup>

The main thing that distinguishes sandwich and monolithic structures lies in the glass serving FTO, the sandwich structure has two glass platforms serving FTO. In contrast, the monolithic structure consists of one FTO-coated glass plate, so that the manufacturing cost is relatively cheaper than sandwich structures.<sup>68</sup> In addition, monolithic dye solar cells are manufactured using a composite layer as a CE. All cells are growing on one substrate.<sup>27</sup> Younas et al<sup>27</sup> reported that highly mesoporous carbon-based electrodes (HMC) are an inexpensive alternative for the high electrocatalytic activity for sandwich structure. The fabrication process for sandwich structure shows energy conversion with the addition of 1% NiO doping in TiO<sub>2</sub> increases the efficiency, and 2% NiO decreases due to the superhydrophilic nature of the material.<sup>82</sup>

Monolithic perovskite solar cells are using TiO<sub>2</sub> nanoparticles. The thickness of the pore layer between TiO<sub>2</sub> and CE in monolithic solar cells affects the efficiency of cell performance.<sup>51</sup> Power conversion and stability of 1000 hours improved quite well, as well as low fabrication costs, the monolithic device structure is a good choice for commercial use.<sup>48</sup>

The difference between sandwich and honeycomb structure is in the shape of the CE. CE affects cell performance through three main functions, namely catalyst, charge collector, and light reflector.<sup>83-85</sup> Graphene has a hexagonal shape resembling honeycomb and has advantages such as high electrical and thermal stability and desired optical and mechanical properties.<sup>73</sup> This material also has high optical transparency, excellent thermal conductivity, high hole mobility, and others, which are very suitable for use as CE.<sup>83,86,87</sup>

The addition of honeycomb-shaped graphene to the semiconducting TiO<sub>2</sub> layer can increase the adsorption photons of dyes. The increase in photons absorption affects the mobility of electrons and consequently improving photovoltaic performance.<sup>23</sup>

## 5 | CONCLUSION, CHALLENGES, AND FUTURE PROSPECTS

The effects of various types of dyes, both synthetic and natural dyes, on the performance of DSSC have been explained and discussed. The investigation of various dyes is an efficient and practical guide for the future development of solar cell technology based dye. Dyes and the shape of the structure play a role in improving the efficiency of DSSC. Dye represents the core component of DSSC and has the function of receiving photons and anode sensitization. We found that synthetic dyes are effective and commonly used in increasing the efficiency

of DSSC compared with that of organic dyes based on ruthenium (Ru) metals such as N719, N3, and N719 + N3. In addition, there is also Indoline (D149) dye quite often used in engineering materials to improve the DSSC performance because of good absorption ability in the visible light region. For natural dyes, better photovoltaic performance is for dyes derived from fruits and vegetables due to the molecular structure of riboflavin, chlorophyll, and carotenoid pigments useful for UV absorption.

The essential part affects the efficiency of DSSC structure. We have reviewed the various structures that make up the DSSC, namely sandwich, monolithic, and honeycomb structures. The monolithic structure exhibits lower efficiency in the traditional (sandwich) configuration due to the isolation, which blocks diffusion. Meanwhile, the honeycomb structure is distinguished from the CE and can develop a new DSSC in the future. The honeycomb structure has a hexagonal honeycomb-shaped CE. This structure shows a much higher conversion than conventional DSSC, which has potential for future direction.<sup>22</sup>

The low cost, environmentally friendly, flexible, and stability of DSSC are prominent and challenges in future research. For mass production, some aspects still need for serious consent in observation and collaborative research. In this regard, some recommendations for future research are as follows:

1. The TiO<sub>2</sub> and FTO-based substrates are the most expensive and rigid part for DSSC. The extensive research is still open to find new flexible conductive substrate with low cost, high electron mobility, large surface area, good light absorption ability, and environmentally friendly. Doping is possible for producing large surface area and increasing the absorption of dyes, which allows more absorption of sunlight so that ECE increases.
2. The research for charge generation and charge transport at the interfacial contact is needed to improve efficiency by controlling the interface band offset. By controlling the band offset, we can easily help the charge transport for reducing the recombination charge, and consequently, increase the performance of DSSC.
3. The essential part in DSSC is dye that is usually used in synthetics compare with that extracted from natural plants. Synthetic dyes use toxic materials and complicated processing. Natural dyes can be easily extracted from the part of the plant such as fruit, flower, and leaves. The natural dyes sources are abundant in nature, easy to prepare, environmentally friendly, and fully biodegradable. The research is needed for improving the stability to be appropriate choice for the long-term use in DSSC.

4. The structure for mass production of DSSC is important. The research for reducing cost by new structure design for flexible DSSC based solid state electrolytes. To understand the interfacial contact and controlling band offset for suppressing recombination charge, the new structure design hopefully much higher conversion than conventional DSSC is need for implementation of mass production.

#### ACKNOWLEDGMENT

This work partially supported by the PD (Penelitian Dasar) and PT (Penelitian Terapan) 2021 grant: 752/UN4.22/PT.01.03/2021 funded by the DIKTI/BRIN, Indonesia.

#### DATA AVAILABILITY STATEMENT

Data available on request from the authors

#### ORCID

Dahlang Tahir <https://orcid.org/0000-0002-8241-3604>

#### REFERENCES

- Karim NA, Mehmood U, Zahid HF, Asif T. Nanostructured photoanode and counter electrode materials for efficient dye-sensitized solar cells (DSSCs). *Sol Energy*. 2019;185:165-188.
- Kumara NTRN, Lim A, Lim CM, Petra MI, Ekanayake P. Recent progress and utilization of natural pigments in dye sensitized solar cells: a review. *Renew Sustain Energy Rev*. 2017;78:301-317.
- Babar F, Mehmood U, Asghar H, et al. Nanostructured photoanode materials and their deposition methods for efficient and economical third generation dye-sensitized solar cells: a comprehensive review. *Renew Sustain Energy Rev*. 2020;129:109919.
- Balachandran K, Kalaivani T, Thangaraju D, Mageswari S, Viswak Senan MS, Preethi A. International conference on newer trends and innovation in mechanical engineering: materials science. *Mater Today Proc*. 2020;37:515-521. <https://doi.org/10.1016/j.matpr.2020.05.485>
- Raguram T, Rajni KS. Effects of varying the soaking duration of Eosin Blue sensitized TiO<sub>2</sub> photoanodes for dye-sensitized solar cells. *Opt Int J Light Electron Opt*. 2020;204:164169.
- Kumar V, Gupta R, Bansal A. Role of chenodeoxycholic acid as co-additive in improving the efficiency of DSSCs. *Sol Energy*. 2020;196:589-596.
- Ferreira BC, Sampaio DM, Suresh Babu R, de Barros ALF. A multi-country analysis on potential adaptive mechanisms to cold and heat in a changing climate. *Opt Mater (Amst)*. 2018;86:239-246.
- Roslan N, Ya'acoba ME, Radzib MAM, Hashimoto Y, Jamaludin D, Chen G. Dye sensitized solar cell (DSSC) greenhouse shading: new insights for solar radiation manipulation. *Renew Sustain Energy Rev*. 2018;92:171-186.
- Gong J, Sumathy K, Qiao Q, Zhou Z. Review on dye-sensitized solar cells (DSSCs): advanced techniques and research trends. *Renew Sustain Energy Rev*. 2017;68:234-246.
- Ejovwokoghene J, Iyuke SE, Daramola M, Oyetunde OA. Synthesis of improved dye-sensitized solar cell for renewable energy power generation. *Sol Energy*. 2020;206:918-934.
- Zatirostami A. Increasing the efficiency of TiO<sub>2</sub>-based DSSC by means of a double layer RF-sputtered thin film blocking layer. *Opt Int J Light Electron Opt*. 2020;207:164419.
- Hemavathi B, Akash S, Shanmukappagouda JK, et al. New 2-methoxy-4,6-bis(4-(4-nitrostyryl)phenyl)nicotinonitrile: Synthesis, characterization and DSSC study. *J Photochem Photobiol A Chem*. 2019;377:75-79.
- Rajamanickam N, Ramachandran K. Improved photovoltaic performance in nano TiO<sub>2</sub> based dye sensitized solar cells: effect of TiCl<sub>4</sub> treatment and Sr doping. *J Colloid Interface Sci*. 2020;580:407-418.
- Das TK, Ilaiyaraja P, Sudakar C. Template assisted nanoporous TiO<sub>2</sub> nanoparticles: the effect of oxygen vacancy defects on photovoltaic performance of DSSC and QDSSC. *Sol Energy*. 2018;159:920-929.
- Khan MI, Sabira M, Mustafa GM, et al. 300 keV cobalt ions irradiations effect on the structural, morphological, optical and photovoltaic properties of Zn doped TiO<sub>2</sub> thin films based dye sensitized solar cells. *Ceram Int*. 2020;46:16813-16819.
- Khan MI, Hassan G, Ramay SM, et al. Investigations on the efficiency variation of zinc and gallium Co-doped TiO<sub>2</sub> based dye sensitized solar cells. *Ceram Int*. 2020;46:24844-24849. <https://doi.org/10.1016/j.ceramint.2020.06.268>
- Dahlan D, Md Saad SK, Berli AU, Bajili A, Umar AA. Synthesis of two-dimensional nanowall of Cu-doped TiO<sub>2</sub> and its application as photoanode in DSSCs. *Phys E Low-Dimens Syst Nanostruct*. 2017;91:185-189.
- Liu J, Li Y, Arumugam S, Tudor J, Beeby S. Investigation of low temperature processed titanium dioxide (TiO<sub>2</sub>) films for printed dye sensitized solar cells (DSSCs) for large area flexible applications. *Mater Today Proc*. 2018;5:13846-13854.
- Gao N, Wan T, Xu Z, Ma L, Ramakrishna S, Liu Y. Nitrogen doped TiO<sub>2</sub>/graphene nanofibers as DSSCs photoanode. *Mater Chem Phys*. 2020;255:123542.
- Naveen Kumar TR, Yuvaraj S, Kavitha P, Sudhakar V, Krishnamoorthy K, Neppolian B. Aromatic amine passivated TiO<sub>2</sub> for dye-sensitized solar cells (DSSC) with ~9.8% efficiency. *Sol Energy*. 2020;201:965-971.
- Ünlü B, Özacar M. Effect of Cu and Mn amounts doped to TiO<sub>2</sub> on the performance of DSSCs. *Sol Energy*. 2020;196:448-456.
- Ali Umar MI, Resti VH, Umar AA. The influence of MoSe<sub>2</sub> coated onto Pt film to DSSC performance with the structure TiO<sub>2</sub>/Dye/LxMoSe<sub>2</sub>Pt (0 ≤ x ≤ 5). *Mater Lett*. 2020;275:3-6.
- Kumar KA, Subalakshmi K, Senthilselvan J. Effect of co-sensitization in solar exfoliated TiO<sub>2</sub> functionalized rGO photoanode for dye-sensitized solar cell applications. *Mater Sci Semi-cond Process*. 2019;96:104-115.
- Ünlü B, Çakar S, Özacar M. The effects of metal doped TiO<sub>2</sub> and dithizone-metal complexes on DSSCs performance. *Sol Energy*. 2018;166:441-449.
- Manikandan VS, Palai AK, Mohanty S, Nayak SK. Hydrothermally synthesized self-assembled multi-dimensional TiO<sub>2</sub>/graphene oxide composites with efficient charge transfer kinetics fabricated as novel photoanode for dye sensitized solar cell. *J Alloys Compd*. 2019;793:400-409.
- Dhas V, Muduli S, Agarkar S, et al. Enhanced DSSC performance with high surface area thin anatase TiO<sub>2</sub> nanoleaves. *Sol Energy*. 2011;85:1213-1219.

27. Younas M, Baroud TN, Gondal MA, Dastageer MA, Giannelis EP. Highly efficient, cost-effective counter electrodes for dye-sensitized solar cells (DSSCs) augmented by highly mesoporous carbons. *J Power Sources*. 2020;468:228359.
28. Guo H, Hu Z, Zhao L, et al. Facile synthesis of chrysanthemum flowers-like TiO<sub>2</sub> hierarchical microstructures assembled by nanotube for high performance dye-sensitized solar cells. *Org Electron*. 2018;55:97-105.
29. Nien YH, Chen HH, Hsu HH, et al. Enhanced photovoltaic conversion efficiency in dye-sensitized solar cells based on photoanode consisting of TiO<sub>2</sub>/GO/Ag nanofibers. *Vacuum*. 2019;167:47-53.
30. He Y, Zhang Z, Wang W, Fu L. Metal organic frameworks derived high-performance photoanodes for DSSCs. *J Alloys Compd*. 2020;825:154089.
31. Desai ND, Khot KV, Dongale T, Musselman KP, Bhosale PN. Development of dye sensitized TiO<sub>2</sub> thin films for efficient energy harvesting. *J Alloys Compd*. 2019;790:1001-1013.
32. Önen T, Karakuş MÖ, Coşkun R, Çetin H. Reaching stability at DSSCs with new type gel electrolytes. *J Photochem Photobiol A Chem*. 2019;385:112082.
33. Sanjay P, Deepa K, Madhavan J, Senthil S. Performance of TiO<sub>2</sub> based dye-sensitized solar cells fabricated with dye extracted from leaves of *Peltophorum pterocarpum* and *Acalypha amentacea* as sensitizer. *Mater Lett*. 2018;219:158-162.
34. Arulraj A, Senguttuvan G, Veeramani S, Sivakumar V, Subramanian B. Photovoltaic performance of natural metal free photo-sensitizer for TiO<sub>2</sub> based dye-sensitized solar cells. *Opt Int J Light Electron Opt*. 2019;181:619-626.
35. Hamadani M, Safaei-Ghomi J, Hosseinpour M, Masoomi R, Jabbari V. Uses of new natural dye photosensitizers in fabrication of high potential dye-sensitized solar cells (DSSCs). *Mater Sci Semicond Process*. 2014;27:733-739.
36. Erande KB, Hawaldar PY, Suryawanshi SR, et al. Extraction of natural dye (specifically anthocyanin) from pomegranate fruit source and their subsequent use in DSSC. *Mater Today Proc*. 2020;43:2716-2720. <https://doi.org/10.1016/j.matpr.2020.06.357>
37. Singh LK, Koiry BP. Natural dyes and their effect on efficiency of TiO<sub>2</sub> based DSSCs: a comparative study. *Mater Today Proc*. 2018;5:2112-2122.
38. Pervez A, Javed K, Iqbal Z, et al. Fabrication and comparison of dye-sensitized solar cells by using TiO<sub>2</sub> and ZnO as photo electrode. *Opt Int J Light Electron Opt*. 2019;182:175-180.
39. Jaafar H, Ahmad ZA, Ain MF. The use of carbon black-TiO<sub>2</sub> composite prepared using solid state method as counter electrode and E. conferta as sensitizer for dye-sensitized solar cell (DSSC) applications. *Opt Mater (Amst)*. 2018;79:366-371.
40. Shalini S, Kumar TS, Prasanna S, Balasundaraprabhu R. Investigations on the effect of co-doping in enhancing the performance of nanostructured TiO<sub>2</sub> based DSSC sensitized using extracts of *Hibiscus Sabdariffa calyx*. *Opt Int J Light Electron Opt*. 2020;212:164672.
41. Shalini S, Balasundaraprabhu R, Kumar TS, et al. Enhanced performance of sodium doped TiO<sub>2</sub> nanorods based dye sensitized solar cells sensitized with extract from petals of *Hibiscus sabdariffa* (Roselle). *Mater Lett*. 2018;221:192-195.
42. Shalini S, Prabavathy N, Balasundaraprabhu R, et al. Studies on DSSC encompassing flower shaped assembly of Na-doped TiO<sub>2</sub> nanorods sensitized with extract from petals of *Kigelia Africana*. *Opt Int J Light Electron Opt*. 2018;155:334-343.
43. Maurya IC, Neetu AKG, Srivastava P, Bahadur L. *Callindra haematocephata* and *Peltophorum pterocarpum* flowers as natural sensitizers for TiO<sub>2</sub> thin film based dye-sensitized solar cells. *Opt Mater (Amst)*. 2016;60:270-276.
44. Ferreira FC, Babu RS, de Barros ALF, Raja S, da Conceição LRB, Mattoso LHC. Photoelectric performance evaluation of DSSCs using the dye extracted from different color petals of *Leucanthemum vulgare* flowers as novel sensitizers. *Spectrochim Acta Part A Mol Biomol Spectrosc*. 2020;233:118198.
45. Mansouri S, Abbaspour-Fard MH, Meshkini A. Lily (*Iris persica*) pigments as new sensitizer and TiO<sub>2</sub> nanofibers as photoanode electrode in dye sensitized solar cells. *Opt Int J Light Electron Opt*. 2020;202:163710.
46. Akila Y, Muthukumarasamy N, Agilan S, Senthilarasu S, Velauthapillai D. Zirconium oxide post treated tin doped TiO<sub>2</sub> for dye sensitized solar cells. *Mater Sci Semicond Process*. 2017;57:24-31.
47. Diantoro M, Maftuha D, Suprayogi T, et al. Performance of *Pterocarpus Indicus* Willd Leaf Extract as Natural Dye TiO<sub>2</sub>-Dye/ITO DSSC. *Mater Today Proc*. 2019;17:1268-1276.
48. Xu L, Wan F, Rong Y, et al. Stable monolithic hole-conductor-free perovskite solar cells using TiO<sub>2</sub> nanoparticle binding carbon films. *Organic Electronics*. 2017;45:131-138.
49. Huang Y, Zhao L, Li Y, Li W, Wang S. Comparison of mesoporous materials based on mixed-organic-cation hole-conductor-free perovskite solar cells. *App Surf Sci*. 2019;493:975-981.
50. Bett AJ, Schulze PSC, Winkler K, et al. Low temperature perovskite solar cells with an evaporated TiO<sub>2</sub> compact layer for perovskite silicon tandem solar cells. *Energy Procedia*. 2017;124:567-576.
51. Xu M, Liu G, Li X, et al. Efficient monolithic solid-state dye-sensitized solar cell with a low-cost mesoscopic carbon based screen printable counter electrode. *Org Electron*. 2013;14:628-634.
52. Jošt M, Albrecht S, Lipovšek B, et al. Back- and front-side texturing for light-management in perovskite / silicon-heterojunction tandem solar cells. *Energy Procedia*. 2016;102:43-48.
53. Li D, Jiang Z, Xia Q, Zhang Z, Yao Z. Efficient homogeneous and isomorphic blocking layer – skeleton rutile TiO<sub>2</sub> electron transfer structure for quantum dot sensitized solar cells. *Results Phys*. 2018;11:1015-1021.
54. Ašmontas S, Anbinderis M, Gradauskas J, et al. Low resistance TiO<sub>2</sub>/p-Si heterojunction for tandem solar cells. *Materials*. 2020;13:2857.
55. Liu H, Fu X, Bala H, et al. An effective TiO<sub>2</sub> blocking layer for hole-conductor-free perovskite solar cells based on carbon counter electrode. *Org Electron*. 2018;59:253-259.
56. Wei W, Björefors F, Nyholm L. Hybrid energy storage devices based on monolithic electrodes containing well-defined TiO<sub>2</sub> nanotube size gradients. *Electrochim Acta*. 2015;176:1393-1402.
57. Apostolopoulou A, Sygkridou D, Rapsomanikis A, Kalarakis AN, Stathatos E. Enhanced performance of meso-structured perovskite solar cells in ambient conditions with a composite TiO<sub>2</sub>-In<sub>2</sub>O<sub>3</sub> electron transport layer. *Solar Energy Mater Solar Cells*. 2017;166:100-107.

58. Haque S, Mendes MJ, Sobrado OS, Águas H, Fortunato E, Martins R. Photonic-structured TiO<sub>2</sub> for high-efficiency, flexible and stable perovskite solar cells. *Nano Energy*. 2019;59:91-101.
59. Baran E, Yazici B. Fabrication of TiO<sub>2</sub>-NTs and TiO<sub>2</sub>-NTs covered honeycomb lattice and investigation of carrier densities in Γ<sup>-</sup>/I<sup>3-</sup> electrolyte by electrochemical impedance spectroscopy. *Appl Surf Sci*. 2015;357:2206-2216.
60. Nada AA, el Roubay WMA, Bekheet MF, et al. Highly textured boron/nitrogen co-doped TiO<sub>2</sub> with honeycomb structure showing enhanced visible-light photoelectrocatalytic activity. *Appl Surf Sci*. 2020;505:144419.
61. Xia G, Liu H, Zhao X, Dong X, Wang S, Li X. Seeding-method-processed anatase TiO<sub>2</sub> film at low temperature for efficient planar perovskite solar cell. *Chem Eng J*. 2019;370:1111-1118.
62. Zhang Y, Lan X, Wang L, Liu P, Zhang Y, Shi J. Novel precursor-reforming strategy to the conversion of honeycomb-like 3DOM TiO<sub>2</sub> to ant nest-like macro-mesoporous N-TiO<sub>2</sub> for efficient hydrogen production. *Sol Energy*. 2019;194:189-196.
63. Wu H, Wang Y, Ma Y, Xiao T, Yuan D, Zhang Z. Honeycombed TiO<sub>2</sub> nanotube arrays with top-porous/bottom-tubular structures for enhanced photocatalytic activity. *Ceram Int*. 2015;41:2527-2532.
64. Iftikhar H, Sonai GG, Hashmi SG, Nogueira AF, Lund PD. Progress on electrolytes development in dye-sensitized solar cells. *Materials*. 2019;12:1998.
65. Shakeel Ahmad M, Pandey AK, Abd Rahim N. Advancements in the development of TiO<sub>2</sub> photoanodes and its fabrication methods for dye sensitized solar cell (DSSC) applications. A review. *Renew Sustain Energy Rev*. 2017;77:89-108.
66. Lee CP, Ho KC. Poly(ionic liquid)s for dye-sensitized solar cells: a mini-review. *Eur Polym J*. 2018;108:420-428.
67. Ahmed U, Alizadeh M, Rahim NA, Shahabuddin S, Ahmed MS, Pandey AK. A comprehensive review on counter electrodes for dye sensitized solar cells: a special focus on Pt-TCO free counter electrodes. *Sol Energy*. 2018;174:1097-1125.
68. Aslam A, Mehmood U, Arshad MH, et al. Dye-sensitized solar cells (DSSCs) as a potential photovoltaic technology for the self-powered internet of things (IoTs) applications. *Sol Energy*. 2020;207:874-892.
69. Behrouznejad F, Taghavinia N, Ghazyani N. Monolithic dye sensitized solar cell with metal foil counter electrode. *Org Electron*. 2018;57:194-200.
70. Takeda Y, Kato N, Higuchi K, et al. Monolithically series-interconnected transparent modules of dye-sensitized solar cells. *Sol Energy Mater and sol Cells*. 2009;93:808-811.
71. Kumar DK, Kr̄iz̄ J, Bennett N, et al. Functionalized metal oxide nanoparticles for efficient dye-sensitized solar cells (DSSCs): a review. *Mater Sci Energy Technol*. 2020;3:472-481.
72. Iqbal MZ, Ali SR, Khan S. Progress in dye sensitized solar cell by incorporating natural photosensitizers. *Sol Energy*. 2019;181:490-509.
73. Li H, Xiao Y, Han G, Zhang Y. A transparent honeycomb-like poly(3,4-ethylenedioxythiophene)/multi-wall carbon nanotube counter electrode for bifacial dye-sensitized solar cells. *Org Electron*. 2017;50:161-169.
74. S. A. Kazmi, S. Hameed, A. S. Ahmed, M. Arshad, and A. Azam, *J. Alloys Compd.*, (2016). <https://doi.org/10.1016/j.jallcom.2016.08.319>, 691, 659, 665.
75. Suriani AB, Muqoyyanah AM, Mamat MH, et al. Improving the photovoltaic performance of DSSCs using a combination of mixed-phase TiO<sub>2</sub> nanostructure photoanode and agglomerated free reduced graphene oxide counter electrode assisted with hyperbranched surfactant. *Opt Int J Light Electron Opt*. 2018;158:522-534. <https://doi.org/10.1016/j.ijleo.2017.12.149>
76. Slimi A, Hachi M, Fitri A, et al. Effects of electron acceptor groups on triphenylamine-based dyes for dye-sensitized solar cells: theoretical investigation. *J Photochem Photobiol A Chem*. 2020;398:112572.
77. Xu Z, Li Y, Li Y, et al. Theoretical study of T shaped phenothiazine/carbazole based organic dyes with naphthalimide as π-spacer for DSSCs. *Spectrochim Acta Part A Mol Biomol Spectrosc*. 2020;233:118201.
78. Bandara TMWJ, DeSilva LA, Ratnasekera JL, et al. High efficiency dye-sensitized solar cell based on a novel gel polymer electrolyte containing RbI and tetrahexylammonium iodide (Hex4NI) salts and multi-layered photoelectrodes of TiO<sub>2</sub> nanoparticles. *Renew Sustain Energy Rev*. 2019;103:282-290.
79. Qamar M, Zhang B, Feng Y. Enhanced photon harvesting in dye-sensitized solar cells by doping TiO<sub>2</sub> photoanode with NaYF<sub>4</sub>:Yb<sup>3+</sup>,Tm<sup>3+</sup> microrods. *Opt Mater (Amst)*. 2019;89:368-374.
80. Sinha D, De D, Goswami D, Mondal A, Ayaz A. ZnO and TiO<sub>2</sub> nanostructured dye sensitized solar photovoltaic cell. *Mater Today Proc*. 2019;11:782-788.
81. Prabavathy N, Balasundaraprabhu R, Balaji G, et al. Investigations on the photo catalytic activity of calcium doped TiO<sub>2</sub> photo electrode for enhanced efficiency of anthocyanins based dye sensitized solar cells. *J Photochem Photobiol A Chem*. 2019;377:43-57.
82. Nakayama K, Luangchaisri C, Muangphat C, Praweerawat K. Preparation of NiO/TiO<sub>2</sub> composite films for enhanced dye sensitized solar cell efficiency. *Mater Today Proc*. 2020;23:690-695.
83. Samantaray MR, Mondal AK, Murugadoss G, et al. Synergetic effects of hybrid carbon nanostructured counter electrodes for dye-sensitized solar cells: a review. *Materials (Basel)*. 2020;13:2779.
84. B. Abdullah, S. Ilyas, D. Tahir, *J Nanomater* 6, 9823263 (2018). <https://doi.org/10.1155/2018/9823263>, Nanocomposites Fe/activated carbon/PVA for microwave absorber: synthesis and characterization, 6
85. Tahir D, Oh SK, Kang HJ, Tougaard S. Composition dependence of dielectric and optical properties of Hf-Zr-silicate thin films grown on Si(100) by atomic layer deposition. *Thin Solid Films*. 2016;616:425-430.
86. Heryanto H, Abdullah B, Tahir D. Analysis of structural properties of X-ray diffraction for composite copper-activated carbon by modified Williamson-Hall and size-strain plotting methods. *J Phys Conf Ser*. 2018;1080:12007.
87. Ilyas S, Abdullah B, Tahir D. Enhancement of absorbing frequency and photo-catalytic performance by temperature treatment of composites Fe<sub>3</sub>O<sub>4</sub>-AC nanoparticle. *Adv Powder Technol*. 2020;31(3):905-913.

**How to cite this article:** Mujtahid F, Gareso PL, Armynah B, Tahir D. Review effect of various types of dyes and structures in supporting performance of dye-sensitized solar cell TiO<sub>2</sub>-based nanocomposites. *Int J Energy Res*. 2022;46(2): 726-742. doi:10.1002/er.7310

# Review effect of various types of dyes and structures in supporting performance of dye-sensitized solar cell TiO<sub>2</sub>-based nanocomposites

## ORIGINALITY REPORT

16%

SIMILARITY INDEX

11%

INTERNET SOURCES

12%

PUBLICATIONS

%

STUDENT PAPERS

## PRIMARY SOURCES

1	<a href="http://onlinelibrary.wiley.com">onlinelibrary.wiley.com</a> Internet Source	1%
2	<a href="http://avesis.cu.edu.tr">avesis.cu.edu.tr</a> Internet Source	1%
3	<a href="http://libmast.utm.my">libmast.utm.my</a> Internet Source	1%
4	<a href="http://dokumen.pub">dokumen.pub</a> Internet Source	1%
5	Burak Ünlü, Soner Çakar, Mahmut Özacar. "The effects of metal doped TiO <sub>2</sub> and dithizone-metal complexes on DSSCs performance", Solar Energy, 2018 Publication	<1%
6	<a href="http://chemistry-europe.onlinelibrary.wiley.com">chemistry-europe.onlinelibrary.wiley.com</a> Internet Source	<1%
7	<a href="http://www.mdpi.com">www.mdpi.com</a> Internet Source	<1%

8

[link.springer.com](https://link.springer.com)

Internet Source

&lt;1 %

9

Omar Britel, Asmae Fitri, Adil Touimi Benjelloun, Ahmed Slimi, Mohammed Benzakour, Mohammed Mcharfi. "Theoretical design of new carbazole based organic dyes for DSSCs applications. A DFT/TD-DFT insight", Journal of Photochemistry and Photobiology A: Chemistry, 2022

Publication

&lt;1 %

10

Vikash Kumar, Renu Gupta, Ajay Bansal. "Role of chenodeoxycholic acid as co-additive in improving the efficiency of DSSCs", Solar Energy, 2020

Publication

&lt;1 %

11

[theses.lib.polyu.edu.hk](https://theses.lib.polyu.edu.hk)

Internet Source

&lt;1 %

12

[preview-nanoscalereslett.springeropen.com](https://preview-nanoscalereslett.springeropen.com)

Internet Source

&lt;1 %

13

[eprints.utm.my](https://eprints.utm.my)

Internet Source

&lt;1 %

14

[www.scilit.net](https://www.scilit.net)

Internet Source

&lt;1 %

15

[ebin.pub](https://ebin.pub)

Internet Source

&lt;1 %

[hdl.handle.net](https://hdl.handle.net)

16

Internet Source

&lt;1 %

17

[tubiblio.ulb.tu-darmstadt.de](https://tubiblio.ulb.tu-darmstadt.de)

Internet Source

&lt;1 %

18

M. Mehedi Hasan, Md Didarul Islam, Taslim Ur Rashid. "Biopolymer-Based Electrolytes for Dye-Sensitized Solar Cells: A Critical Review", *Energy & Fuels*, 2020

Publication

&lt;1 %

19

[acta.bibl.u-szeged.hu](https://acta.bibl.u-szeged.hu)

Internet Source

&lt;1 %

20

"Counter Electrodes for Dye-sensitized and Perovskite Solar Cells", Wiley, 2018

Publication

&lt;1 %

21

[arxiv.org](https://arxiv.org)

Internet Source

&lt;1 %

22

Falak Babar, Umer Mehmood, Hafza Asghar, M. Hassan Mehdi, Anwar Ul Haq Khan, Hamza Khalid, Noor ul Huda, Zaira Fatima.

"Nanostructured photoanode materials and their deposition methods for efficient and economical third generation dye-sensitized solar cells: A comprehensive review", *Renewable and Sustainable Energy Reviews*, 2020

Publication

&lt;1 %

23	<a href="http://ujcontent.uj.ac.za">ujcontent.uj.ac.za</a> Internet Source	<1 %
24	<a href="http://www.jscholaronline.org">www.jscholaronline.org</a> Internet Source	<1 %
25	<a href="http://www.science.gov">www.science.gov</a> Internet Source	<1 %
26	<a href="http://www.semanticscholar.org">www.semanticscholar.org</a> Internet Source	<1 %
27	Azimah Omar, Mohd Syukri Ali, Nasrudin Abd Rahim. "Electron transport properties analysis of titanium dioxide dye-sensitized solar cells (TiO <sub>2</sub> -DSSCs) based natural dyes using electrochemical impedance spectroscopy concept: A review", Solar Energy, 2020 Publication	<1 %
28	M. Hamadani, J. Safaei-Ghomi, M. Hosseinpour, R. Masoomi, V. Jabbari. "Uses of new natural dye photosensitizers in fabrication of high potential dye-sensitized solar cells (DSSCs)", Materials Science in Semiconductor Processing, 2014 Publication	<1 %
29	<a href="http://flex.flinders.edu.au">flex.flinders.edu.au</a> Internet Source	<1 %
30	K. Balachandran, T. Kalaivani, D. Thangaraju, S. Mageswari, M.S. Viswak Senan, A. Preethi.	<1 %

"Fabrication of photoanodes using sol-gel synthesized Ag-doped TiO<sub>2</sub> for enhanced DSSC efficiency", Materials Today: Proceedings, 2021

Publication

31

Yanfeng He, Zhenyu Zhang, Weiyang Wang, Lipei Fu. "Metal organic frameworks derived high-performance photoanodes for DSSCs", Journal of Alloys and Compounds, 2020

Publication

<1 %

32

[epdf.pub](http://epdf.pub)

Internet Source

<1 %

33

[iopscience.iop.org](http://iopscience.iop.org)

Internet Source

<1 %

34

[openaccess.altinbas.edu.tr](http://openaccess.altinbas.edu.tr)

Internet Source

<1 %

35

"Solar Cells", Springer Science and Business Media LLC, 2020

Publication

<1 %

36

[www.degruyter.com](http://www.degruyter.com)

Internet Source

<1 %

37

Ishwar Chandra Maurya, Shalini Singh, Pankaj Srivastava, Biswajit Maiti, Lal Bahadur.

"Natural dye extract from Cassia fistula and its application in dye-sensitized solar cell: Experimental and density functional theory studies", Optical Materials, 2019

<1 %

38

K. Ashok Kumar, K. Subalakshmi, J. Senthilselvan. "Effect of co-sensitization in solar exfoliated TiO<sub>2</sub> functionalized rGO photoanode for dye-sensitized solar cell applications", Materials Science in Semiconductor Processing, 2019

Publication

<1 %

---

39

Paweł Gnida, Marcin Libera, Agnieszka Pająk, Ewa Schab-Balcerzak. "Examination of the Effect of Selected Factors on the Photovoltaic Response of Dye-Sensitized Solar Cells", Energy & Fuels, 2020

Publication

<1 %

---

40

Cigdem Sahin, Canan Varlikli. "Chapter 25 Visible Range Activated Metal Oxide Photocatalysts in New and Emerging Energy Applications", Springer Science and Business Media LLC, 2022

Publication

<1 %

---

41

Muhammad Ahsan Saeed, Hyeong Cheol Kang, Kicheon Yoo, Francis Kwaku Asiam, Jae-Joon Lee, Jae Won Shim. "Cosensitization of metal-based dyes for high-performance dye-sensitized photovoltaics under ambient lighting conditions", Dyes and Pigments, 2021

Publication

<1 %

---

42 Nayab Abdul Karim, Umer Mehmood, Hafiza Fizza Zahid, Tahira Asif. "Nanostructured photoanode and counter electrode materials for efficient Dye-Sensitized Solar Cells (DSSCs)", Solar Energy, 2019  
Publication <1 %

---

43 [api.crossref.org](https://api.crossref.org)  
Internet Source <1 %

---

44 [journals.lww.com](https://journals.lww.com)  
Internet Source <1 %

---

45 "Interfacial Engineering in Functional Materials for Dye - Sensitized Solar Cells", Wiley, 2019  
Publication <1 %

---

46 "Photoenergy and Thin Film Materials", Wiley, 2019  
Publication <1 %

---

47 [WWW.mdpi.com](https://www.mdpi.com)  
Internet Source <1 %

---

48 Zhonghai Zhang, Yanjie Yu, Peng Wang. " Hierarchical Top-Porous/Bottom-Tubular TiO Nanostructures Decorated with Pd Nanoparticles for Efficient Photoelectrocatalytic Decomposition of Synergistic Pollutants ", ACS Applied Materials & Interfaces, 2012  
Publication <1 %

---

49	<a href="http://depositonce.tu-berlin.de">depositonce.tu-berlin.de</a> Internet Source	<1 %
50	<a href="http://epdf.tips">epdf.tips</a> Internet Source	<1 %
51	<a href="http://mdpi-res.com">mdpi-res.com</a> Internet Source	<1 %
52	<a href="http://newestech.com">newestech.com</a> Internet Source	<1 %
53	<a href="http://repository.unhas.ac.id">repository.unhas.ac.id</a> Internet Source	<1 %
54	<a href="http://worldwidescience.org">worldwidescience.org</a> Internet Source	<1 %
55	<a href="http://www.osapublishing.org">www.osapublishing.org</a> Internet Source	<1 %
56	<a href="http://www.readkong.com">www.readkong.com</a> Internet Source	<1 %
57	A. Arulraj, G. Senguttuvan, S. Veeramani, V. Sivakumar, B. Subramanian. "Photovoltaic performance of natural metal free photosensitizer for TiO <sub>2</sub> based dye-sensitized solar cells", Optik, 2019 Publication	<1 %
58	Guijiao Xia, Hongli Liu, Xiaoming Zhao, Xiaofei Dong, Shirong Wang, Xianggao Li. "Seeding-method-processed anatase TiO <sub>2</sub> film at low	<1 %

temperature for efficient planar perovskite solar cell", Chemical Engineering Journal, 2019

Publication

---

59

Kerttu Aitola, Jinbao Zhang, Nick Vlachopoulos, Janne Halme et al. "Carbon nanotube film replacing silver in high-efficiency solid-state dye solar cells employing polymer hole conductor", Journal of Solid State Electrochemistry, 2015

Publication

---

60

Lanling Zhao, Guochen Wang, Yanbing Liu, Zhenqing Yang. "First principles design novel D5 derivative dyes with excellent acceptors for highly efficient dye-sensitized solar cells", Computational and Theoretical Chemistry, 2021

Publication

---

61

Mohamed Elhousseini Hilal, Abdelkhalk Aboulouard, Abdul Rehman Akbar, Hussein A. Younus, Nesrin Horzum, Francis Verpoort. "Progress of MOF-Derived Functional Materials Toward Industrialization in Solar Cells and Metal-Air Batteries", Catalysts, 2020

Publication

---

62

Ningxiao Gao, Tingting Wan, Zhiyang Xu, Liansheng Ma, Seeram Ramakrishna, Yong Liu. "Nitrogen doped TiO<sub>2</sub>/Graphene

<1 %

<1 %

<1 %

<1 %

# nanofibers as DSSCs photoanode", Materials Chemistry and Physics, 2020

Publication

63

Ruby Baby, Peter Daniel Nixon, Nallapaneni Manoj Kumar, M. S. P. Subathra, Nallamuthu Ananthi. "A comprehensive review of dye-sensitized solar cell optimal fabrication conditions, natural dye selection, and application-based future perspectives", Environmental Science and Pollution Research, 2021

Publication

<1 %

64

Wu, Guohua, Fantai Kong, Yaohong Zhang et al. "Multiple-Anchoring Triphenylamine Dyes for Dye-Sensitized Solar Cell Application", The Journal of Physical Chemistry C

Publication

<1 %

65

[journal.hep.com.cn](http://journal.hep.com.cn)

Internet Source

<1 %

66

[mrs.org](http://mrs.org)

Internet Source

<1 %

67

[nepis.epa.gov](http://nepis.epa.gov)

Internet Source

<1 %

68

[pubs.rsc.org](http://pubs.rsc.org)

Internet Source

<1 %

69

Kai Zhu, Nathan R. Neale, Alexander Miedaner, Arthur J. Frank. "Enhanced Charge-

<1 %

## Collection Efficiencies and Light Scattering in Dye-Sensitized Solar Cells Using Oriented TiO Nanotubes Arrays ", Nano Letters, 2007

Publication

---

70

Jihuai Wu, Zhang Lan, Jianming Lin, Miaoliang Huang, Yunfang Huang, Leqing Fan, Genggeng Luo. "Electrolytes in Dye-Sensitized Solar Cells", Chemical Reviews, 2015

Publication

---

<1 %

71

Kuan-Yu Lin, Ming-Quan Cai, Yu-Ting Wu, Min-Hsin Yeh, Jyh-Chiang Jiang. "Boron and Nitrogen Codoped Multilayer Graphene as a Counter Electrode: A Combined Theoretical and Experimental Study on Dye-Sensitized Solar Cells under Ambient Light Conditions", The Journal of Physical Chemistry C, 2021

Publication

---

<1 %

---

Exclude quotes      On

Exclude matches      < 5 words

Exclude bibliography      On